Tuning the Palladium−Silicon Bond: Bond Analysis of Bisphosphine Silyl Palladium Hydrides

Heiko Jacobsen* and Mark J. Fink*

Department of Chemistry, Tulane University, New Orleans, Louisiana 70118

Received October 18, 2005

Density functional calculations (PW91) have been carried out for 33 complexes of the type (dhpe)M(H)Si(R^1)(R^2)(R^3) (dhpe = 1,2-bis(dihydrophosphino)ethane; M = Pd, Pt; R = H, Me, Ph, F, Cl). Bond snapping energies for the M−Si bond have been obtained, and the variation of silyl substitutents R allows one to tune the M−Si bond strength over a range of about 60 kJ/mol. On the basis of the results obtained from a Hirshfeld charge analysis, the Pd−Si bond is characterized by a sizable amount of charge transfer from the transition-metal fragment to the main-group ligand. This is reflected in the optimized Pd−Si bond length, which correlates well with the amount of charge transferred. Experimentally observed trends for the relative stability of bisphosphine silyl palladium hydrides can be successfully reproduced using a simplified approximation based on reaction energies derived from bond snapping energies. On average, the Pt−Si bond is stronger than the Pd−Si bond by 26 kJ/mol. The enhanced platinum bond strengths relative to those of palladium are attributed to relativistic effects.

1. Introduction

The prominent role that palladium plays as an effective catalyst in a variety of organic transformations[1] has spawned a plethora of theoretical and computational studies.[2] The aim of these studies centers on the elucidation of the bonding situation in palladium complexes and the clarification of the mechanisms of palladium-mediated catalytic transformations. Since the key step in many catalytic transformations is often an oxidative addition or reductive elimination process, the study of palladium-mediated C−C or C−H bond cleavage[3] and C−C or C−O bond formation[4,5] is a prime focal point of computational investigations.

Whereas the main body of transition-metal (TM)-mediated catalytic processes is centered around the TM−carbon or TM−hydrogen bond, TM−silyl chemistry has grown immensely over the past two decades[6] and palladium-catalyzed reactions of hydrosilanes are involved in a number of important synthetic methodologies.[7] Stable silyl palladium complexes are rare,[8] but a class of simple bis(silyl) palladium complexes has been synthesized, bearing the chelating dcpe ligand (dcpe = 1,2-bis(dicyclohexylphosphino)ethane).[9] Recently, the first examples of the mononuclear palladium silyl hydrides (dcpe)Pd(H)SiR_3 have been reported, again containing the sterically demanding dcpe ligand.[10] These complexes are stereochemically nonrigid[11] through fluxional processes which may parallel the steps involved in C−H reductive elimination.

In view of the prominent and promising role of palladium as an agent in key transformations in synthetic chemistry, we have undertaken a computational study of square-planar silyl palladium hydrides for a variety of silyl ligands. The mechanistic aspects of oxidative addition of saturated Si−H bonds to Pd(PH_3)$_2$ and Pt(PH_3)$_2$ have been theoretically analyzed in detail by Sakaki and co-workers.[12] However, since it has long been realized that TM−hydrogen and TM−carbon bond strengths can be considered as "the keys to catalysis",[13] the main focus of the present study is on the palladium−silicon bond, specifically on bond strength and substitution patterns that allow for a suitable tuning of the palladium−silicon bond. It is hoped that the present theoretical study will provide valuable insights into the nature of the palladium−silicon bond and will be helpful when developing new strategies for extending the realm of palladium catalysis with respect to silicon-based transformations. We further compare the bonding situation for palladium to its heavier congener platinum, identifying the factors responsible for the significant difference between palladium−silicon and platinum−silicon chemistry. Before we discuss our results in more detail, we will present a brief account of the computational strategy employed in this work.

* To whom correspondence should be addressed. E-mail: jacobsen@kemkom.com (H.J.); fink@tulane.edu (M.J.F.).

(1) Fiaud, J. C.; Malleron, J.-L.; Legros, J. Y. *Handbook of Palladium-Catalyzed Organic Reactions: Synthetic Aspects and Catalytic Cycles*; Academic Press: New York, 1997.

(2) Dedieu, A. *Chem. Rev.* **2000**, *100*, 543−600.

(3) (a) Diefenbach, A.; Bickelhaupt, F. M. *J. Phys. Chem. A* **2004**, *108*, 8460−8466. (b) Diefenbach, A.; de Jong, G. T.; Bickelhaupt, F. M. *J. Chem. Theor. Comput.* **2005**, *1*, 286−298.

(4) Ananikov, V. P.; Musaev, D. G.; Morokuma, K. *Organometallics* **2005**, *24*, 715−723.

(5) Zuidema, E.; van Leuwen, P. W. N. M.; Bo, C. *Organometallics* **2005**, *24*, 3703−3710.

(6) Corey, J. Y.; Braddock-Wilking, J. *Chem. Rev.* **1999**, *99*, 175−292.

(7) Tsuji, J.; *Palladium Reagents and Catalysts: New Perspectives for the 21st Century*; Wiley: New York, 2004.

(8) (a) Curtis, M. D.; Greene, J. *J. Am. Chem. Soc.* **1978**, *100*, 6362−6367. (b) Eaborn, C.; Griffiths, R. W.; Pidcock, A. *J. Organomet. Chem.* **1982**, *225*, 331−341. (c) Seyferth, D.; Goldman, E. W.; Escudie, J. *J. Organomet. Chem.* **1984**, *271*, 337−352. (d) Schubert, U.; Müller, C. *J. Organomet. Chem.* **1989**, *373*, 165−172.

(9) (a) Pan, Y.; Mague, J. T.; Fink, M. J. *Organometallics* **1992**, *11*, 3495−3497. (b) Pan, Y.; Mague, J. T.; Fink, M. J. *J. Am. Chem. Soc.* **1993**, *115*, 3842−3843.

(10) Boyle, R. C.; Mague, J. T.; Fink, M. J. *J. Am. Chem. Soc.* **2003**, *125*, 3228−3229.

(11) Muetterties, E. L. *Acc. Chem. Res.* **1970**, *3*, 266−273.

(12) (a) Sakaki, S.; Masami, I. *J. Am. Chem. Soc.* **1993**, *115*, 2373−2381. (b) Sakaki, S.; Ogawa, M.; Kinoshita, M. *J. Phys. Chem.* **1995**, *99*, 9933−9939.

(13) Martinho Simões, J. A.; Beauchamp, J. L. *Chem. Rev.* **1990**, *90*, 629−688.

10.1021/om050901m CCC: $33.50
Publication on Web 03/18/2006

Chart 1

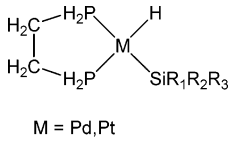

M = Pd,Pt

Table 1. Summary of Palladium and Platinum Complexes (dhpe)M(H)Si(R^1)(R^2)(R^3) Considered in This Work

compd	M	R^1	R^2	R^3	compd	M	R^1	R^2	R^3
1a	Pd	H	H	H	**1r**	Pd	H	Ph	Cl
1b	Pd	Me	Me	Me	**1s**	Pd	H	Ph	F
1c	Pd	Ph	Ph	Ph	**1t**	Pd	Me	Ph	Cl
1d	Pd	Cl	Cl	Cl	**1u**	Pd	Me	Ph	F
1e	Pd	F	F	F	**1v**	Pd	Me	Ph	Ph
1f	Pd	H	H	Me	**2a**	Pt	H	H	H
1g	Pd	H	H	Ph	**2b**	Pt	Me	Me	Me
1h	Pd	H	H	Cl	**2c**	Pt	Ph	Ph	Ph
1i	Pd	H	H	F	**2d**	Pt	Cl	Cl	Cl
1j	Pd	H	Me	Me	**2e**	Pt	F	F	F
1k	Pd	H	Ph	Ph	**2f**	Pt	H	H	Me
1l	Pd	H	Cl	Cl	**2g**	Pt	H	H	Ph
1m	Pd	H	F	F	**2h**	Pt	H	H	Cl
1n	Pd	Me	Me	Ph	**2i**	Pt	H	H	F
1o	Pd	Me	Me	Cl	**2n**	Pt	Me	Me	Ph
1p	Pd	Me	Me	F	**2v**	Pt	Ph	Ph	Me
1q	Pd	H	Ph	Me					

2. Computational Details

Gradient-corrected density functional calculations employing exchange and correlation corrections proposed by Perdew and Wang[14] have been performed with the Amsterdam Density Functional suite of programs, ADF version 2004.01.[15] The valence electrons of Pd, Pt, and Si were described with ADF basis set IV (triple-ζ STO plus one polarization function), and for the remaining atoms ADF basis set III (double-ζ STO plus one polarization function) was chosen. Electrons of the core shells (1s2s2p3s3p3d for Pd; 1s2s2p3s3p3d4s4p4d4f for Pt; 1s2s2p for Si, P, and Cl; 1s for C and F) have been treated within the frozen-core approximation. If not noted otherwise, relativistic effects have been incorporated on the basis of the zero-order regular approximation.[16] It has been demonstrated that explicit consideration of relativistic effects is of importance for the quantum chemical description of oxidative addition reactions of palladium.[17]

3. Results and Discussion

3.1. Model Systems. Geometries of 33 complexes of the type (dhpe)M(H)Si(R^1)(R^2)(R^3) have been optimized, which are schematically depicted in Chart 1, and summarized in Table 1 (dhpe = 1,2-bis(dihydrophosphino)ethane).

The dhpe ligand has been chosen as a model system for the dcpe ligand, and a representative optimized geometry for complex **1c** is presented in Figure 1. The model geometry can be compared to the experimentally determined structure of the related complex (dcpe)Pd(H)$SiPh_3$ (**3a**). The agreement between experimental geometry and calculated structure is reasonably good. A structural agreement of similar quality also is found between the optimized geometry of complex **2c** and the crystal structure of the related complex (dcpe)Pt(H)$SiPh_3$ (**4**).[18] Therefore, the set of model complexes should provide good data for a qualitative assessment of general trends for the palladium− and platinum−silicon bonds.

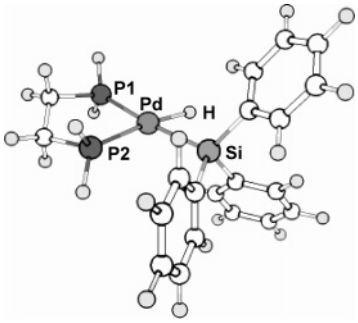

Figure 1. Optimized geometry of model complex **1c**. Relevant bond distances (in pm) and angles (in deg) in comparison with experimental values for (dcpe)Pd(H)$SiPh_3$ (**3c**) (in parentheses, from the X-ray structure reported in ref 10): Pd−Si, 236 (233); Pd−P1, 237 (235); Pd−P2, 232 (232); Pd−H, 162; Si−Pd−P1, 170 (166); Si−Pd−H, 63.

For the palladium systems, both the experimental geometry and the calculated structure show two significantly different Pd−P bond lengths, the phosphorus atom being in a position trans to the silyl ligand exhibiting the longer metal−ligand separation. The same structural motif, although less pronounced, is also observed for the platinum complexes. The elongated M−P bond trans to silicon (M = Pd, Pt) is consistent with the known high trans influence attributed to silyl groups.[19] Similar observations with respect to different Pd−P bond lengths were also made by Sakaki and co-workers.[12]

3.2. Reductive Elimination of Palladium Model Systems. The stability of silyl palladium hydrides is strongly dependent on the substitution pattern of the silyl ligand, and equilibria represented by eq 1 have been investigated by NMR for the complexes (dcpe)Pd(H)$SiPh_3$ (**3a**), (dcpe)Pd(H)$SiPh_2Me$ (**3b**), (dcpe)Pd(H)$SiPhMe_2$ (**3c**), and (dcpe)Pd(H)$SiEt_3$ (**3d**).

$$(\text{dcpe})\text{PdH}(\text{SiR}_3) + \text{HSiR}'_3 \rightleftharpoons (\text{dcpe})\text{PdH}(\text{SiR}'_3) + \text{HSiR}_3 \quad (1)$$

The experiments resulted in a relative stability order of **3a** > **3b** > **3c** > **3d**, with K_{eq} values relative to **3d** of 2400:310:24:1.[10]

To investigate the influence of silyl substitution, we have calculated reaction energies ΔE_{RE} as changes in total bond energy for the reductive elimination represented by eq 2.

$$(\text{dhpe})\text{PdH}(\text{SiR}_3) \rightarrow (\text{dhpe})\text{Pd} + \text{HSiR}_3 \quad (2)$$

The results of this analysis are presented in Figure 2. The reaction energies ΔE_{RE} range from 81 kJ/mol for the trimethyl-substituted complex **1b** to 126 kJ/mol for the trichloro model complex **1d**. The data collected in Figure 2 indicate that substitution of hydrogen by a halogen or a phenyl group leads

(14) (a) Perdew, J. P.; Chevary, J. A.; Vosko, S. H.; Jackson, K. A.; Pederson, M. R.; Singh, D. J.; Fiolhais, C. *Phys. Rev. B* **1992**, *46*, 6671−6687. (b) Perdew, J. P.; Wang, Y. *Phys. Rev. B* **1992**, *45*, 13244−13249.

(15) (a) Baerends, E. J.; Ellis, D. E.; Ros, P. *Chem. Phys.* **1973**, *2*, 41−51. (b) Versluis, L.; Ziegler, T. *J. Chem. Phys.* **1988**, *88*, 322−328. (c) Guerra, C. F.; Snijders, J. G.; te Velde, G.; Baerends, E. J. *Theor. Chem. Acc.* **1998**, *99*, 391−403. (d) te Velde, G.; Bickelhaupt, F. M.; Baerends, E. J.; Guerra, C. F.; Van Gisbergen, S. J. A.; Snijders, J. G.; Ziegler, T. *J. Comput. Chem.* **2001**, *22*, 931−967.

(16) (a) van Lenthe, E.; Baerends, E. J.; Snijders, J. G. *J. Chem. Phys.* **1993**, *99*, 4597−4610. (b) van Lenthe, E.; Baerends, E. J.; Snijders, J. G. *J. Chem. Phys.* **1994**, *101*, 9783−9792. (c) van Lenthe, E.; van Leeuwen, R.; Baerends, E. J.; Snijders, J. G. *Int. J. Quantum Chem.* **1996**, *57*, 281−293. (d) van Lenthe, E.; Ehlers, A.; Baerends, E. J. *J. Chem. Phys.* **1999**, *110*, 8943−8953.

(17) Diefenbach, A.; Bickelhaupt, F. M. *J. Chem. Phys.* **2001**, *115*, 4030−4040.

(18) Boyle, R. C. The Interaction of Palladium(0) Complexes with Silanes. Ph.D. Thesis, Tulane University, 2003.

(19) Coe, B. J.; Glenright, S. J. *Coord. Chem. Rev.* **2000**, *203*, 5−80.

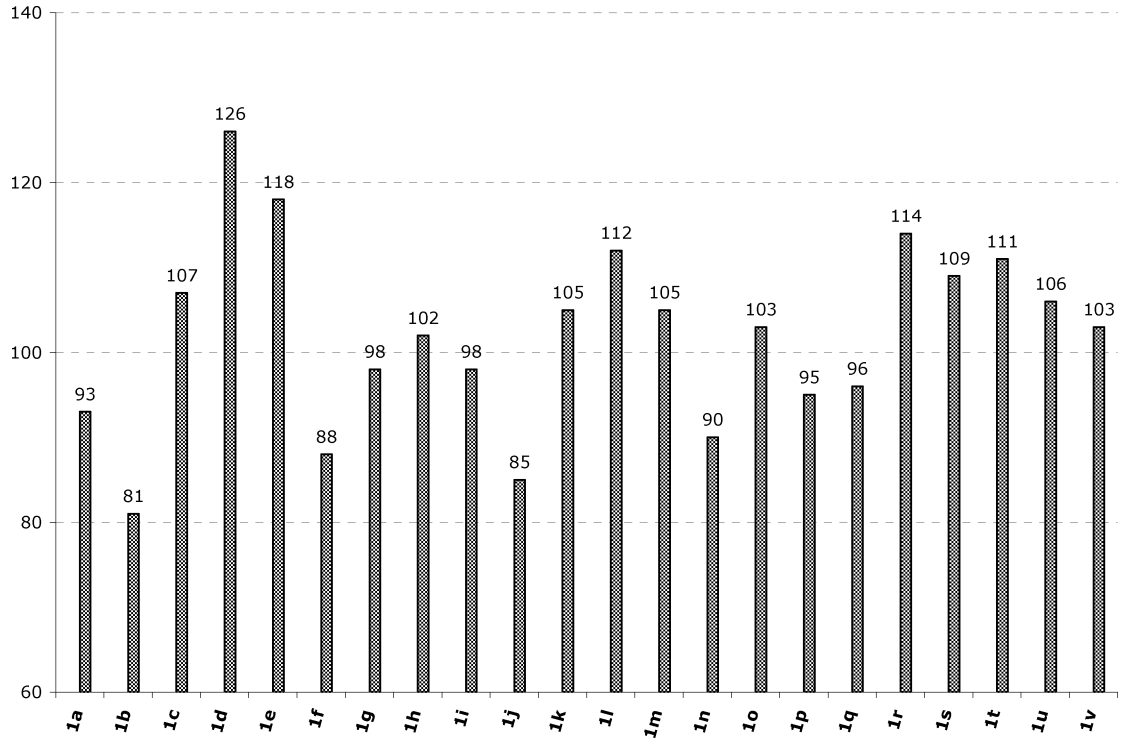

Figure 2. Reaction energies of reductive elimination ΔE_{RE} (in kJ/mol) for the palladium-based model complexes **1a**−**v**.

to an increase in reaction energy, whereas methyl groups cause the opposite effect.

Under the assumption that the difference in free energies of reaction is mainly determined by the difference in strength of the bonds broken and formed, one can use the reaction energies to estimate relative equilibrium constants at room temperature for the process represented in eq 3. Considering complexes

$$(\text{dhpe})\text{PdH}(\text{SiR}_3) + \text{HSiR}'_3 \rightleftharpoons (\text{dhpe})\text{PdH}(\text{SiR}'_3) + \text{HSiR}_3 \quad (3)$$

(dhpe)Pd(H)$SiMe_3$ (**1b**), (dhpe)Pd(H)$SiPh_3$ (**1c**), and (dcpe)Pd(H)$SiPhMe_2$ (**1n**), a relative stability order of **1c** > **1v** > **1n** > **1b** is obtained, with K_{eq} values relative to **1b** of 36 000:7200:38:1. This result is in satisfactory qualitative agreement with the experimental values.

The data presented in Figure 2 further suggest that the effect of silyl substituents is additive. Considering the complexes **1a**−**e**, one can derive SiR increments for ΔE_{RE}, which amount to 31 kJ/mol (R = H), 27 kJ/mol (R = Me), 36 kJ/mol (R = Ph), 42 kJ/mol (R = Cl), and 39 kJ/mol (R = F), respectively. The reaction energies for complexes **1f**−**u** based on these increments are in good agreement with the calculated values, with a root-mean-square value of 3 kJ/mol. In general, larger deviations are observed for the chlorine- and fluorine-containing complexes, whereas in cases when the silyl ligand carries only carbon- and hydrogen-based substituents the agreement is close within 2 kJ/mol.

3.3. Bond Analysis of the Pd−Si Bond. To get a better understanding of the nature of the palladium−silicon bond, a bond analysis was performed which is based on the fragment approach to chemical bonding. To this end, we make use of a well-established bond partitioning scheme,[20,21] which breaks down the bond between two fragments into various contributions from different interactions. In particular, we look at the bond-forming reaction between the transition-metal fragment and the silyl ligand. The palladium−silicon bond is then built up by the interaction of two suitably prepared fragments, having the right geometry of the final molecule and an electron configuration that allows for the formation of a proper doubly occupied bonding orbital. This interaction is shown in Scheme 1, and the energy associated with this bond-forming reaction is referred to as the bond snapping energy, BE_{snap}.[22] Although BE_{snap} values are not defined in the same way as bond dissociation enthalpies ΔH, they are reasonable approximations of bond enthalpy terms, which in turn provide a good description for the bond strength.[13]

Scheme 1

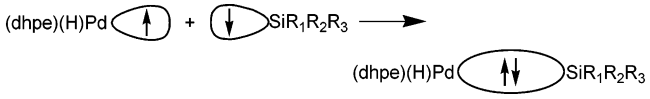

The energy associated with the reaction depicted in Scheme 1 can be partitioned into two main components, namely a term due to steric repulsion, ΔE^0, and an orbital interaction term, ΔE_{int} (eq 4).

$$BE_{snap} = -[\Delta E^0 + \Delta E_{int}] \quad (4)$$

When two suitable bond-forming fragments are brought together to adapt the geometry of the final molecule, the steric repulsion term includes the classical Coulomb interaction between the unmodified and interpenetrating charge distributions of the two fragments, as well as Pauli repulsion, which takes into account destabilizing two-orbital−four-electron interactions between occupied orbitals on both fragments. The term ΔE_{int} introduces the attractive orbital interaction between occupied and virtual orbitals on the two fragments and includes polarization and charge-transfer contributions.

(20) Ziegler, T. *NATO ASI Ser.* **1992**, *No. C378*, 367−391.
(21) Bickelhaupt, F. M.; Baerends, E. J. *Rev. Comput. Chem.* **2000**, *15*, 1−86.
(22) Jacobsen, H.; Ziegler, T. *Comments Inorg. Chem.* **1995**, *17*, 301−317.

Table 2. Bond Analysis for the Pd−Si Bonds of Model Complexes 1a−v[a]

compd	R^1, R^2, R^3	ΔE^0	ΔE_{int}	BE_{snap}
1e	F, F, F	38	−411	373
1m	H, F, F	86	−433	347
1d	Cl, Cl, Cl	78	−423	345
1s	H, Ph, F	62	−404	342
1t	Me, Ph, Cl	53	−393	340
1u	Me, Ph, F	50	−390	340
1c	Ph, Ph, Ph	59	−394	335
1o	Me, Me, Cl	47	−382	335
1i	H, H, F	95	−429	334
1r	H, Ph, Cl	68	−402	334
1p	Me, Me, F	39	−372	333
1k	H, Ph, Ph	66	−398	332
1v	Me, Ph, Ph	47	−379	332
1l	H, Cl, Cl	103	−432	329
1q	H, Ph, Me	55	−383	328
1h	H, H, Cl	89	−414	325
1g	H, H, Ph	70	−393	323
1×bb	H, H, H	63	−384	321
1n	Me, Me, Ph	57	−378	321
1f	H, H, Me	58	−378	320
1j	H, Me, Me	52	−370	318
1b	Me, Me, Me	49	−365	316

[a] All energy values are given in kJ/mol.

The results of the Pd−Si bond analysis for model complexes **1a**−**u** are collected in Table 2. It is instructive to first analyze the homosubstituted systems [Pd]−SiR_3 (R = H, Me, Ph, Cl, F; [Pd] = (dhpe)Pd(H)). The following ranking is observed for the bond snapping energy BE_{snap}: F > Cl > Ph > H >Me. The silyl ligand carrying the more strongly electron withdrawing substituents, due to either electronegativity or electron delocalization onto the R substituents, forms a stronger silyl−palladium bond. In fact, out of the 21 palladium complexes investigated, the complex [Pd]−SiF_3 (**1e**) displays the strongest Pd−Si bond, whereas the complex [Pd]−$SiMe_3$ (**1b**) shows the weakest Pd−Si interaction. When the contributions to BE_{snap} are considered individually, one finds the following ranking for the stabilizing orbital interaction ΔE_{int}: Cl > F > Ph > H > Me. The order for the destabilizing steric repulsion ΔE^0 is Cl > H > Ph >Me > F. In general, the trend in destabilizing steric repulsions parallels the trend in orbital interaction, with the noticeable exception of the compound [Pd]−SiF_3 (**1e**). Although compound **1e** forms the strongest Pd−Si bond, it does not display the strongest orbital interaction but a noticeably reduced steric repulsion. Due to the highly electronegative fluorine substituents on the silyl ligand, the electron cloud of the silyl ligand is mainly localized at the R substituents. This reduces the destabilizing two-orbital/four-electron interactions between the palladium and the silyl fragments.

When analyzing orbital interactions and steric contributions for the complexes with heterosubstituted silyl ligands as compared to the homosubstituted systems, one finds that a number of compounds carrying hydrogen-substituted silyl ligands such as **1g**−**i**,**l**,**m** show a remarkable increase in both steric repulsion as well as orbital interaction. For example, the complex [Pd]−$SiHF_2$ (**1m**) shows an orbital interaction exceeding the value of [Pd]−SiF_3 (**1m**) and a steric repulsion that is significantly larger than the value for [Pd]−SiH_3 (**1a**). Thus, the Pd−Si bond in **1m** does not resemble that of its parent compounds **1a**,**f**. This suggests that for the interaction between the palladium and silyl fragments other secondary bonding interactions in addition to Pd−Si bonding are of importance, such as interaction of the hydride ligand of the palladium fragment with the silyl center. A closer inspection of the optimized geometries should provide further evidence that corroborates the above proposal, and we will now turn to a structural analysis of the palladium model complexes.

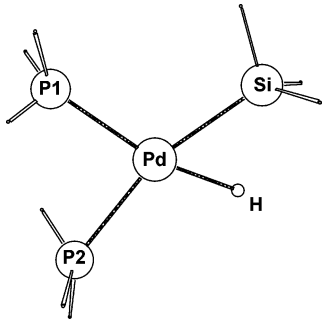

Figure 3. Representative geometry around the transition-metal center for palladium-based model complexes **1a**−**v**.

Table 3. Geometric Parameters (Bond Distances in pm, Angles in deg) for the Hydride Ligands of Model Complexes 1a−v

compd	R^1, R^2, R^3	*d*(Pd−H)	*d*(Si···H)	∠(H−Pd−Si)
1i	H, H, F	163.7	189.7	52.6
1m	H, F, F	163.6	191.1	53.6
1a	H, H, H	162.4	199.5	55.7
1h	H, H, Cl	162.4	200.0	56.5
1f	H, H, Me	162.7	202.3	56.9
1l	H, Cl, Cl	161.9	203.1	58.2
1g	H, H, Ph	162.6	203.3	57.4
1b	Me, Me, Me	162.6	203.4	56.8
1j	H, Me, Me	162.7	204.1	57.4
1n	Me, Me, Ph	162.6	205.4	57.7
1e	F, F, F	161.7	206.8	60.3
1q	H, Ph, Me	162.9	207.0	58.9
1s	H, Ph, F	163.2	209.3	60.5
1k	H, Ph, Ph	162.3	212.3	61.1
1u	Me, Ph, F	162.9	212.7	61.6
1p	Me, Me, F	162.8	214.4	62.0
1c	Ph, Ph, Ph	161.8	216.7	62.7
1o	Me, Me, Cl	162.3	218.6	63.9
1r	H, Ph, Cl	162.0	219.0	64.2
1t	Me, Ph, Cl	162.2	223.0	65.7
1v	Me, Ph, Ph	161.9	223.4	65.2
1d	Cl, Cl, Cl	160.3	232.8	70.2

3.4. Geometries of Pd−Si Model Complexes. In Figure 3, a representative geometry around the transition-metal center is displayed, together with the nomenclature used to define bond distances and bond angles.

We begin with an analysis of the coordination geometry of the hydride ligand, and relevant geometric parameters are collected in Table 3. For model complexes **1a**−**u**, the value for the Pd−H bond is fairly constant and ranges from 160 to 164 pm. However, the Si−H separation changes significantly from 190 pm for complex **1i** to 233 pm for complex **1d**. The trend observed in the bond analysis of hydrogen-substituted silyl ligands is reflected in the Si−H separation: complexes that show both increased steric repulsion and increased orbital interaction display a short Si−H distance. Good examples for this trend are compounds **1i**,**m**. We further note that hydrogen-substituted silyl ligands in general show short Si−H distances, whereas chlorine-substituted silyl ligands display large values for the Si−H separation.

The coordination geometry of the hydride ligand supports the notion that secondary Si−H bonding interactions are of importance for palladium silyl hydrides, in accord with the nature of the bonding interaction between the silyl and palladium fragments. Although the variations in Pd−H bond length are not pronounced, they too support the notion of Si−H interactions; complexes with long Si−H distances show short Pd−H

Table 4. Pd−Si and Pd−P Bond Distances (in pm) of Model Complexes 1a−v

compd	R^1, R^2, R^3	*d*(Pd−Si)	*d*(Pd−P1)	*d*(Pd−P2)
1d	Cl, Cl, Cl	231.6	232.7	235.6
1e	F, F, F	232.0	232.0	237.2
1r	H, Ph, Cl	233.8	231.4	236.9
1t	Me, Ph, Cl	233.8	231.0	237.3
1s	H, Ph, F	234.1	230.2	237.7
1o	Me, Me, Cl	234.3	230.7	237.9
1u	Me, Ph, F	234.7	230.4	237.9
1l	H, Cl, Cl	234.7	232.2	237.7
1p	Me, Me, F	235.5	230.3	238.4
1m	H, F, F	235.6	231.0	238.7
1k	H, Ph, Ph	236.2	232.2	237.3
1v	Me, Ph, Ph	236.3	231.7	236.8
1c	Ph, Ph, Ph	236.3	232.0	237.2
1h	H, H, Cl	236.9	231.8	237.5
1q	H, Ph, Me	237.1	230.2	236.7
1i	H, H, F	237.6	230.6	237.7
1g	H, H, Ph	237.6	231.3	236.6
1f	H, H, Me	238.5	230.7	236.7
1j	H, Me, Me	238.7	230.4	236.8
1a	H, H, H	239.0	231.6	236.4
1n	Me, Me, Ph	239.3	230.7	237.1
1b	Me, Me, Me	240.1	230.7	237.2

bond lengths, whereas complexes with additional Si−H bonding interactions display an elongated Pd−H bond. We also note that the trend in H−Si separation is paralleled in the H−Pd−Si angle; a short *d*(Si···H) distance is accompanied by a small value for the angle ∠(H−Pd−Si).

We now turn to Pd−Si as well as Pd−P bond lengths, the values for which are compiled in Table 4. Beginning with the Pd−P bond length, we find only slight variations of about 2 pm in Pd−P separation in different model complexes. All complexes display the general coordination motif of a shorter Pd−P1 and a longer Pd−P2 bond. An inspection of the molecular orbitals MO_{Pd-Si} and MO_{Pd-H}, which provide the major contributions to the Pd−Si and Pd−H bonds, respectively, holds an explanation for this observation. Relevant orbitals are depicted in Figure 4. MO_{Pd-Si} is not only responsible for the Pd−Si bonding interaction but also carries an antibonding Pd−P2 contribution (Figure 1a). In contrast, MO_{Pd-H} does not contain any antibonding Pd−P contributions. It is the antibonding Pd−P contribution in MO_{Pd-Si} that gives rise to two Pd−P bonds of significantly different bond length.

We find larger variations in the values for the Si−Pd bond, ranging from 232 to 240 pm. Although the values for the Pd−Si bond length correlate fairly well with the reaction energies ΔE_{RE}, there is no apparent direct relation between the bond snapping energies BE_{snap} or its components ΔE^0 and ΔE_{int} with values for *d*(Pd−Si). This again is due to the fact the bond analysis as performed in the present work does not clearly isolate one major bonding interaction but contains contributions from minor interactions as well. We therefore need to identify another bonding criterion that describes the character of the Pd−Si bond, and to this end we have performed a charge analysis of the interaction between palladium and silyl fragments.

3.5. Charge Analysis for the Pd−Si Bond. Here, we consider the net charge flow when the palladium−silicon bond is formed, on the basis of a Hirshfeld charge analysis.[23] The properties and use of Hirshfeld charges have recently been discussed in the context of other charge models,[24] and we only present a brief outline of the concept. The Hirshfeld charge analysis is based on the electron density as a function of space, and it makes use of the electron density of the molecule and of a fictitious promolecule. When using Hirshfeld charges in bond analysis, the promolecule density is defined as the sum of the densities of the interacting fragments, and Hirshfeld charges |*q*| are assigned for each of the interacting fragments, which then describe the net charge flow associated with bond formation. The charge partitioning according to Hirshfeld also provides the basis for an *atom in molecules* (AIM) definition, a concept that bears many important implications for chemistry. The Hirshfeld partitioning scheme has recently been critically analyzed in the context of an AIM interpretation.[25]

Hirshfeld charges |*q*| together with values for *d*(Pd−Si) are depicted in Figure 5. The charge analysis in all cases indicates a net charge flow from the palladium fragment to the silyl ligand, thus indicating a polar Pd−Si bond. It is evident that the Hirshfeld charges |*q*| correlate well with the bond distance Pd−Si; a large value for net charge flow corresponds to a short Pd−Si bond separation. The polarity of the Pd−Si bond is directly reflected in the Pd−Si bond length.

3.6. Comparison of Palladium and Platinum Complexes. Selected geometric parameters for the platinum model complexes are collected in Table 5. Again, we find the structural motif of a long and a short Pt−P bond length. However, the difference in bond length is not as pronounced as it is for the Pd complexes. Variations in values for the Pt−Si bond lengths follow the same trend as observed for the Pd−Si separation, and the calculated Pt−Si and Pd−Si bond lengths for corresponding complexes are the same within 1 pm. All nine platinum model complexes display metal−hydride bond lengths between 161 and 162 pm, again comparable with bond lengths calculated for corresponding Pd−H bonds. All complexes show a long Si···H separation between 257 and 263 pm and H−Pd−Si angles between 77 and 81°. Thus, the coordination geometry of the hydride ligand is markedly different for platinum complexes than it is for palladium complexes; the H−Pd−Si angle is less acute, and the hydride and silyl center are well separated. In contrast to the palladium model compounds, the optimized geometries for complexes **2a**−**i** do not suggest an additional secondary bonding interaction between the hydride ligand and the silicon center.

For the palladium compounds **1a**−**v**, we have seen irregularities in trends of ΔE^0 and ΔE_{int} that suggest the presence of secondary bonding interactions. We will now turn to the bonding

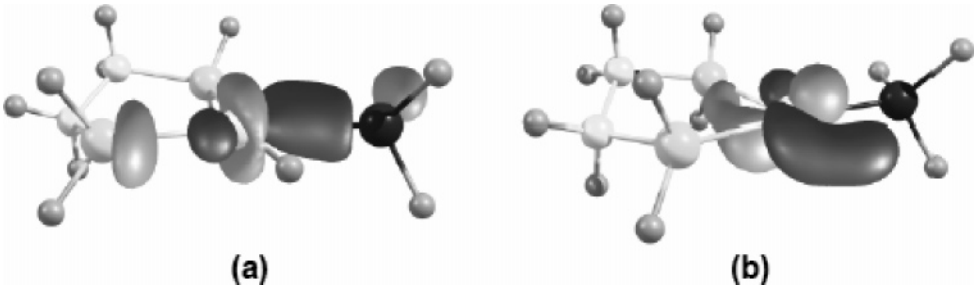

Figure 4. Depiction of molecular orbitals of [Pd]−SiR_3 complexes that represent the (a) Pd−Si bond and (b) Pd−H bond.

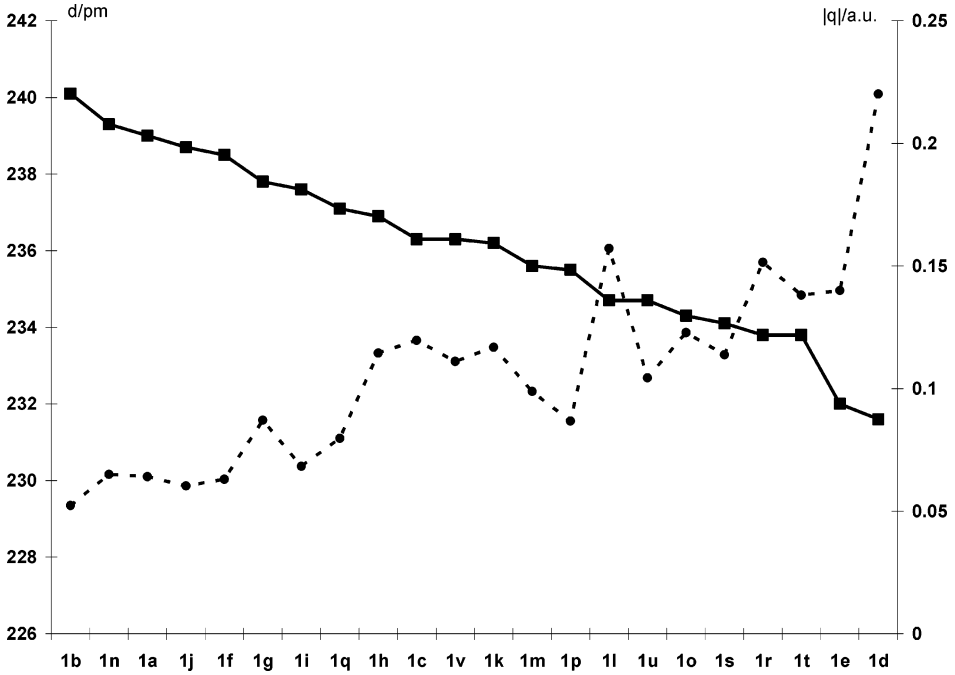

Figure 5. Pd−Si bond lengths d (■, solid line, in pm) and Hirshfeld charges $|q|$ (●, broken line, in au) for palladium-based model complexes **1a**−**v**.

Table 5. Selected Geometric Parameters (Bond Lengths in pm, Angles in deg) for the Platinum Model Complexes (dhpe)Pt(H)Si(R^1) R^2)(R^3) (2a−i,n,v)

compd	R^{1,2}, R^3	d(Pt−Si)	d(Pt−H)	d(Si···H)	∠(H−Pt−Si)	d(Pt−P1)	d(Pt−P2)
2a	H, H	238.9	161.7	257.4	77.3	229.8	232.7
2b	Me, Me	239.6	162.0	256.9	76.8	229.3	234.0
2c	Ph, Ph	238.0	161.8	262.9	79.8	231.2	233.4
2d	Cl, Cl	233.6	161.4	263.4	81.4	231.6	232.3
2e	F, F	233.5	161.5	259.3	79.8	230.8	233.3
2f	H, Me	239.0	161.5	259.4	78.0	229.6	233.4
2g	H, Ph	238.0	161.7	263.1	79.9	231.0	233.3
2h	H, Cl	237.4	161.4	259.5	78.6	230.8	233.7
2i	H, F	237.2	161.4	258.9	78.5	230.4	234.5
2n	Me, Ph	239.4	161.9	263.3	79.4	229.6	233.8
2v	Ph, Me	238.3	161.9	263.3	79.8	230.7	233.7

analysis of platinum model compounds to get a more detailed understanding of the nature of the Pt−Si bond.

Values for BE_{snap} and its components ΔE^0 and ΔE_{int} for the Pt−Si bond in model complexes **2a**−**i** are compiled in Table 6. The same qualitative trends derived for the Pd−Si bond generally hold for the Pt−Si bond as well. However, the exceptional increase in both steric repulsion and orbital interaction which is observed for the palladium complexes **1g**−**i** is not found for the corresponding platinum complexes **2g**−**i**. This supports the notion that, unlike the case for the palladium complexes, secondary bonding interactions between the hydride ligand and the silicon center are not likely as important for platinum complexes. We note that the platinum−silyl bond is stronger than the Pd−Si bond by about 25 kJ/mol. This suggests that the platinum complexes display a different chemistry compared to the palladium compounds. One might expect that the platinum complexes are more stable and less prone to fluxional and stereochemically nonrigid behavior.

For the reductive elimination of platinum model complexes, we further calculated reaction energies ΔE_{RE} as change in total

Table 6. Bond Analysis for the Pt−Si Bonds of Model Complexes 2a−i,n,v[a]

compd	R^{1,2}, R^3	ΔE^0	ΔE_{int}	BE_{snap}
2e	F, F	18	−422	404
2d	Cl, Cl	85	−463	378
2c	Ph, Ph	51	−413	362
2v	Ph, Me	42	−400	358
2i	H, F	39	−395	356
2h	H, Cl	53	−404	351
2g	H, Ph	53	−402	349
2a	H, H	30	−376	346
2n	Me, Ph	34	−378	344
2f	H, Me	29	−372	343
2b	Me, Me	25	−363	338

[a] All energy values are given in kJ/mol.

bond energy, according to the reaction illustrated in eq 5.

$$(\text{dhpe})\text{PtH}(\text{SiR}_3) \rightarrow (\text{dhpe})\text{Pt} + \text{HSiR}_3 \qquad (5)$$

The results are presented in Figure 6, together with values for the related palladium compounds. On average, the reaction energy ΔE_{RE} is 95 kJ/mol larger for Pt systems than it is for Pd systems. Again, considering the complexes **2a**−**e**, one can derive SiR increments for ΔE_{RE}, which amount to 62 kJ/mol (R = H), 27 kJ/mol (R = Me), 67 kJ/mol (R = Ph), 75 kJ/mol (R = Cl), and 72 kJ/mol (R = F), respectively. When the reaction increments for Pd and Pt compounds are compared, the increments for Pt are consistently larger by 31 kJ/mol (R = H, Me, Ph) and 33 kJ/mol (R = Cl, F). This observation supports the notion of an inherent transition-metal effect on the energetics of reductive elimination. The reaction energies for complexes **2f**−**i** and **2n**,**v** based on these increments are in good agreement with the calculated values from eq 5.

The difference in ΔE_{RE}(Pd) and ΔE_{RE}(Pt) is mainly determined by the difference in M−H and M−Si bond strengths. However, one has to keep in mind that for bond strength as commonly understood in a given chemical context, the assump-

(23) Hirshfeld, F. L. *Theor. Chim. Acta* **1977**, *44*, 129−138.
(24) Fonseca Guerra, C.; Handgraaf, J. W.; Baerends, E. J.; Bickelhaupt, F. M. *J. Comput. Chem.* **2004**, *25*, 189−210.
(25) Parr, R. G.; Ayers, P. W.; Nalewajski, R. F. *J. Phys. Chem. A* **2005**, *109*, 3957−3959.

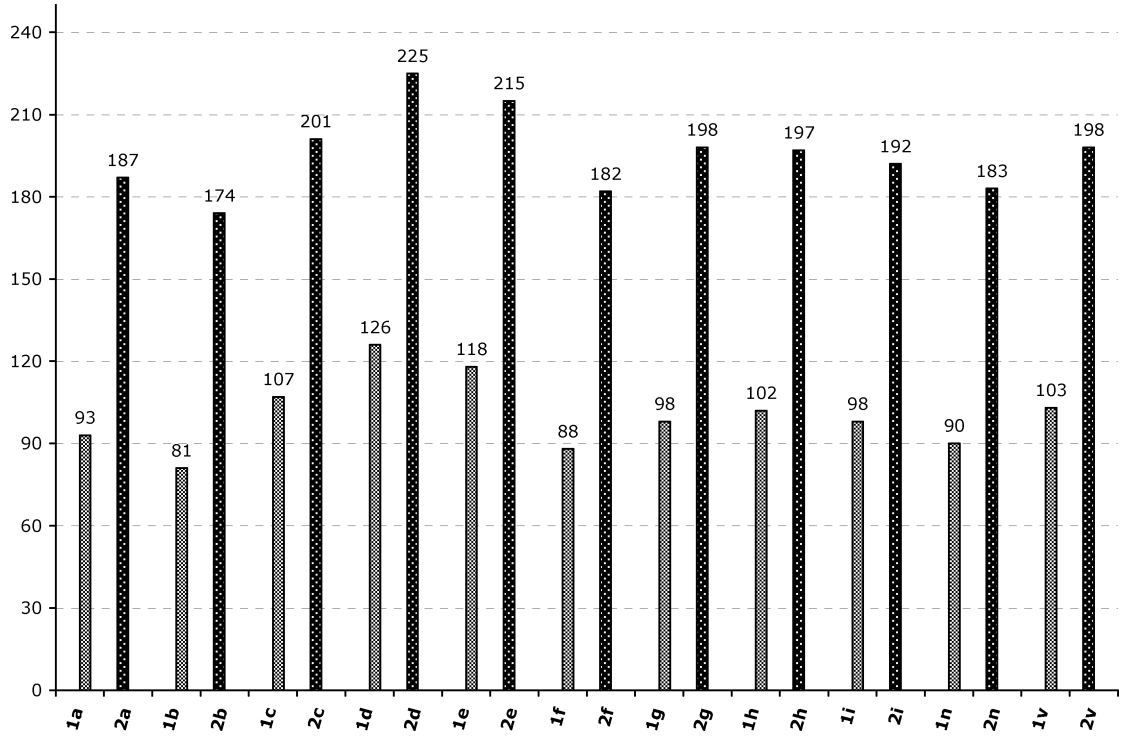

Figure 6. Reaction energies of reductive elimination ΔE_{RE} (in kJ/mol) for the platinum-based model complexes **2a**−**i**,**n**,**v** and for the corresponding palladium compounds.

tion that the sum of the difference in bond strengths equals the difference in reaction energies does not hold (eq 6).

$$BE_{snap}(Pt{-}H) + BE_{snap}(Pt{-}Si) - BE_{snap}(Pd{-}H) - BE_{snap}(Pd{-}Si) \neq \Delta E_{RE}(Pt) - \Delta E_{RE}(Pd) \quad (6)$$

Formally during reductive elimination two metal−ligand bonds are broken, and cleavage of a metal−ligand bond in a first step requires a different amount of energy than cleavage in a second step. For example, the M−H bond strength in (dcpe)MH(SiR_3) is different than the bond strength in (dcpe)MH•.

We will briefly address the differences in M−Si and M−H bond strength in the next section, in the context of differences in Pd−R and Pt−R bond strengths. A detailed analysis of the M−H bond, however, is out of the scope of the present work, and we refer the reader to the literature for a survey of computational studies on transition metal hydrides.[26]

3.7. Relativistic Effects in Pd−Si and Pt−Si Bonding. In the last section, we want to identify reasons why the nature of the platinum−silicon bond significantly differs from that of its lighter palladium-based congener. The answer to the above-posed question is to be found in the explicit consideration of relativistic effects. By now, it is recognized that relativistic effects play a special role considering the nature of chemical bonding,[27] especially in the area of inorganic and organometallic chemistry.[28,29] As already noted, the importance of relativistic effects for calculations of palladium compounds has been stressed in the literature.[17] When a bond analysis is performed according to the scheme introduced above, the origin of relativistic effects becomes apparent, and we shall compare a regular relativistic analysis with a nonrelativistic analysis, explicitly excluding the energy terms that introduce relativistic corrections. An exemplary analysis is performed for the compounds (dhpe)Pd(H)(SiH_3) (**1a**) and (dhpe)Pt(H)(SiH_3) (**2a**) on the basis of their optimized geometries, including relativity. In this context, we will also consider a bond analysis of the transition-metal−hydride bond. The results of these analyses are collected in Table 7. The bond analyses presented in Table 7 reveal the nature of relativistic stabilization, namely an increase in orbital interaction ΔE_{int} as well as a decrease in steric repulsion ΔE^0. The first effect is due to a shift in orbital energies as well as enhanced orbital overlap, whereas the second effect is due to relativistic contraction of the electronic core. The relativistic stabilization of the M−Si bond amounts to 11 kJ/mol for Pd and 55 kJ/mol for Pt. It is this effect that renders the Pt−Si bond stronger than the Pd−Si bond by 23 kJ/mol. The effect observed for the M−Si bond is also the same as that found for the M−H bond, and as a consequence the platinum−hydride bond is stronger than the palladium−hydride bond by 27 kJ/mol. We note that the bond snapping energies for M−Si and M−H bonds are comparable, the latter one being slightly stronger by 12 kJ/mol.

Table 7. Relativistic and Nonrelativistic Bond Analysis for the M−Si and M−H Bonds of Model Complexes 1a and 2a[a]

		M−Si			M−H		
		ΔE^0	ΔE_{int}	BE_{snap}	ΔE^0	ΔE_{int}	BE_{snap}
Pd	rel	63	−384	322	19	−349	330
	nonrel	65	−376	311	24	−342	338
Pt	rel	30	−376	345	−12	−345	357
	nonrel	45	−336	290	17	314	297

[a] All energy values are given in kJ/mol.

Relativistic effects not only influence the strength of transition-metal to ligand bonds but also have a significant influence when the geometries of transition-metal complexes are predicted. In Figure 7, optimized geometries for model compounds **1a** and **2a** with and without explicit consideration of relativistic effects are presented.

(26) Maseras, F., Lledos, A.; Clot, E.; Eisenstein, O. *Chem. Rev.* **2000**, *100*, 601−636.
(27) Pyykkö, P. *Chem. Rev.* **1988**, *88*, 563−594.
(28) Pyykkö, P. *Chem. Rev.* **1997**, *97*, 597−636.
(29) Kaltsoyannis, N. *J. Chem. Soc., Dalton Trans.* **1997**, 1−11.

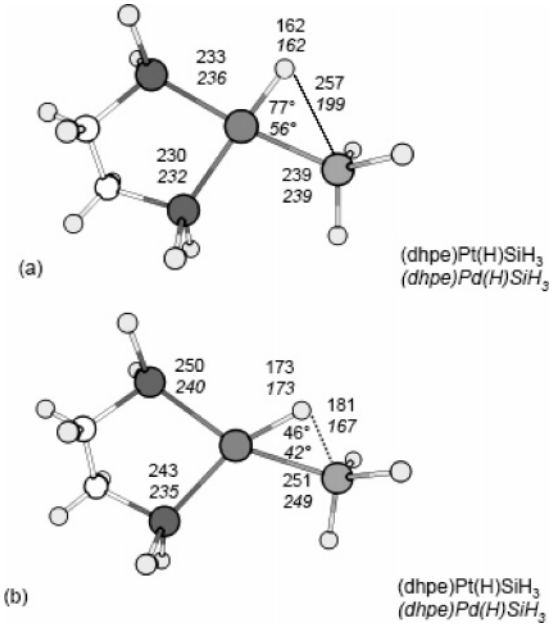

Figure 7. Optimized geometries for the model complexes (dhpe)-Pd(H)SiH_3 (**1a**) and (dhpe)Pt(H)SiH_3 (**2a**) with (a) and without (b) explicit consideration of relativistic effects.

Relativity does not only lead to a significant reduction of the M−L bond lengths but also influences the coordination geometry of the transition-metal hydride ligand. Whereas the relativistic calculations result in compounds with well-separated hydride and silyl ligands, the nonrelativistic calculations predict a substantially smaller H−Pd−Si angle as well as a small H···Si separation. This holds true not only for the platinum complex but also for the palladium compound. Whereas the Pd−Si and Pd−H *bond energies* are fairly well approximated in nonrelativistic calculations, the *nature* of the Pd−H and Pd−Si bond changes significantly when relativistic contributions are either included or omitted. These results support the notion brought forward by Bickelhaupt that relativistic effects are crucial for a proper quantum chemical description of palladium compounds.[17]

4. Conclusion

The calculations presented in this work suggest that variation of silyl substituents R in (dhpe)M(H)Si(R^1)(R^2)(R^3)complexes (M = Pd, Pt) allows one to tune the M−Si bond strength over a range of about 60 kJ/mol. Alkyl-substituted silyl ligands, $R^1 = R^2 = R^3$ = Me, form the weakest bonds, whereas the introduction of both aryl and halogen ligands leads to an increase in the M−Si bond strength. The bond snapping energy is influenced by both orbital interactions and steric repulsion, and the silyl ligands that display the largest orbital interaction do not necessarily form the strongest metal−ligand bond. The Pd−Si bond is characterized by a sizable amount of charge transfer from the transition-metal fragment to the main-group ligand. The Pd−Si bond length serves as an indicator, as it correlates well with the amount of charge transferred.

The difference in bond strength has a direct influence on the energetics of the reductive elimination/oxidative addition of silanes to a bisphosphine transition-metal fragment. The experimentally observed trends for relative stability of bisphosphine silyl palladium hydrides can be successfully reproduced in a simplified approximation based on reaction energies derived from bond snapping energies.

When palladium and platinum complexes are compared, it is found that the latter form stronger M−Si bonds. This in turn has significant influence on the energetics of the reductive elimination/oxidative addition of silanes. The reaction energies for platinum complexes are larger by about 90−100 kJ/mol. The main reason for the differences in bond strength has been argued in terms of relativistic effects, which however are already of significance for palladium complexes.

The results presented in this work not only provide a detailed picture of the nature of the Pd−Si and Pt−Si bonds but also raise questions as to the nature of the Pd−H and Pt−H bonds. The presence of secondary bonding interactions has been noted but has been neither discussed nor analyzed in great detail. Currently, experimental and computational work on the fluxional behavior of palladium hydride complexes is being carried out in our laboratories, and issues relating to the nature of the transition-metal−hydride bond in bisphosphine silyl palladium hydrides are central aspects of our ongoing research.

Acknowledgment. We thank Prof. L. Cavallo for providing access to the MoLNaC Computing Facilities at the Dipartimento di Chimica, Università di Salerno. We also thank DOE/EPSCOR (Grant No. DE-FG-ϕ3ER46046) for financial assistance.

OM050901M